Sputtering-induced vacancy cluster formation on TiO_2(110)

P. Karmakar,* G. F. Liu, and J. A. Yarmoff†
Department of Physics and Astronomy, University of California, Riverside, California 92521, USA
(Received 25 May 2007; revised manuscript received 20 September 2007; published 28 November 2007)

Defects are introduced on an atomically clean TiO_2(110) surface in a controllable manner via bombardment by 0.5 keV Ar^+ ions, and the resultant material is probed with scanning tunneling microscopy and x-ray photoelectron spectroscopy. It is shown that ion bombardment leads to a change of stoichiometry and the formation of vacancy clusters, while annealing after prolonged bombardment forms regular rectangular cavities with single-atomic-layer steps. It is concluded that curvature-dependent sputtering in combination with adatom and vacancy diffusion is responsible for the observed structures.

DOI: 10.1103/PhysRevB.76.193410 PACS number(s): 61.80.Jh, 66.30.Pa, 81.16.−c, 68.47.Gh

Titanium dioxide (TiO_2) is one of the most studied metal oxides due to its use as an efficient photocatalytic material and as a support for catalytically active metal nanoclusters. It has been speculated that defects play a role in many of the applications of TiO_2. Ti vacancies at or near the surface were identified as the active sites for water adsorption, which leads to water splitting.[1] Oxygen vacancies serve as nucleation sites for metal nanocluster growth.[2] It has also been shown that defects are crucial in the interaction of NO with TiO_2.[3] The roughness of the TiO_2 surface increases the hydrophilicity, a property applied in automobile mirrors.[4] Defects on any TiO_2-like metal oxide surface may influence other chemical reactions, so that manipulation of the nature and density of defects could provide a means for controlling the activity. The ability to reproducibly create and characterize defects is rare, however.[5] The defects observed on TiO_2 are generally either intrinsic[6] or produced during cleaning or annealing[7] or by uv radiation.[4]

Sputtering with low-energy ion beams is a common method for the processing and analysis of solid surfaces. Ion beams could also be used to reproducibly generate atomic level defects and nanometer-scale vacancy clusters in a controlled manner. Sputtered TiO_2 has been previously analyzed with surface-sensitive techniques, such as x-ray photoelectron spectroscopy (XPS), Auger electron spectroscopy, low-energy ion scattering (LEIS),[8,9] near-edge x-ray absorption fine structure,[10] and static secondary ion mass spectrometry,[11] which all show sputtering-induced changes in the composition and chemical state.[8]

Recently, much attention has been drawn to nanostructure formation by ion sputtering various materials, since the ion beam parameters, ion-surface geometry, and substrate temperature provide the ability to control the shape and size of the structures formed. Nanocavities have been produced on single-crystal metal surfaces by sputtering.[12,13] A change in the corrugation of the oxide support occurred when Pt on TiO_2 was sputtered at high temperature, indicating that the process depends upon the surface concentration of Pt crystallites.[14] Wang *et al.*[15] observed vacancy clustering in TiO_2 during 2 MeV Au^{2+} ion implantation at elevated temperature and subsequent annealing. Karmarkar *et al.* sputtered a thin Au film on TiO_2, demonstrating the formation of Au nanoclusters with quantum size effects.[16]

In the present work, nanometer-size vacancy clusters are created by Ar^+ sputtering TiO_2(110) and regular rectangular nanocavities are formed by postannealing. The production of such structures on TiO_2(110) by low-energy ion beams has not been reported previously to our knowledge. Prolonged sputtering at room temperature forms vacancy clusters that extend into the material. These structures likely result from a combination of curvature-dependent sputtering and adatom and/or vacancy diffusion. The diffusion occurring at room temperature may be thermal or ion-beam induced. Annealing following significant bombardment recovers the stoichiometry of the TiO_2 surface and produces rectangular-shaped vacancy clusters with atomic layer steps. The presence of the ion-induced cavities and an energy barrier at the step edges are likely responsible for the formation of the rectangular structures.

The experiments were performed in an ultrahigh-vacuum chamber with a base pressure of 1×10^{-10} Torr. A TiO_2(110) single crystal (Commercial Crystal Labs) was attached to a Ta sample holder and annealed by electron beam heating from behind. An infrared pyrometer monitored the temperature. The crystal was prepared by cycles of ion bombardment and annealing (500 eV Ar^+ for 10 min, 975 K for 10 min) until a sharp (1×1) low-energy electron diffraction pattern was obtained and XPS showed no contamination.[17] The TiO_2 was then sputtered at room temperature by normally incident 0.5 keV Ar^+ (current density=1 μA cm^{-2}) at various ion fluences. XPS spectra and scanning tunneling microscope (STM) images were collected after each sputtering and post-annealing step. The images were collected with an *in situ* Park Scientific STM (Autoprobe VT) in constant current mode with a tunneling current of 1 nA and a sample bias of −1.5 V.

The morphology of clean and ion sputtered TiO_2 at various Ar^+ fluences is shown in the STM images of Fig. 1. The terraces and steps of the virgin TiO_2(110) surface are visible in Fig. 1(a), which is similar to the report of Fischer *et al.*[18] Figure 1(b) was collected after bombardment by 3.3×10^{16} ions cm^{-2} of Ar^+, and shows defects and nanometer-scale cavities. Following prolonged bombardment, the vacancies are elongated along the $[1\bar{1}0]$ direction and extend into the subsurface layer, as seen in Fig. 1(c). The average depth of the cavities in each STM image and the fraction of the surface covered by the cavities, i.e., the hole area, are plotted as functions of sputtering fluence in Fig. 1(d). Note

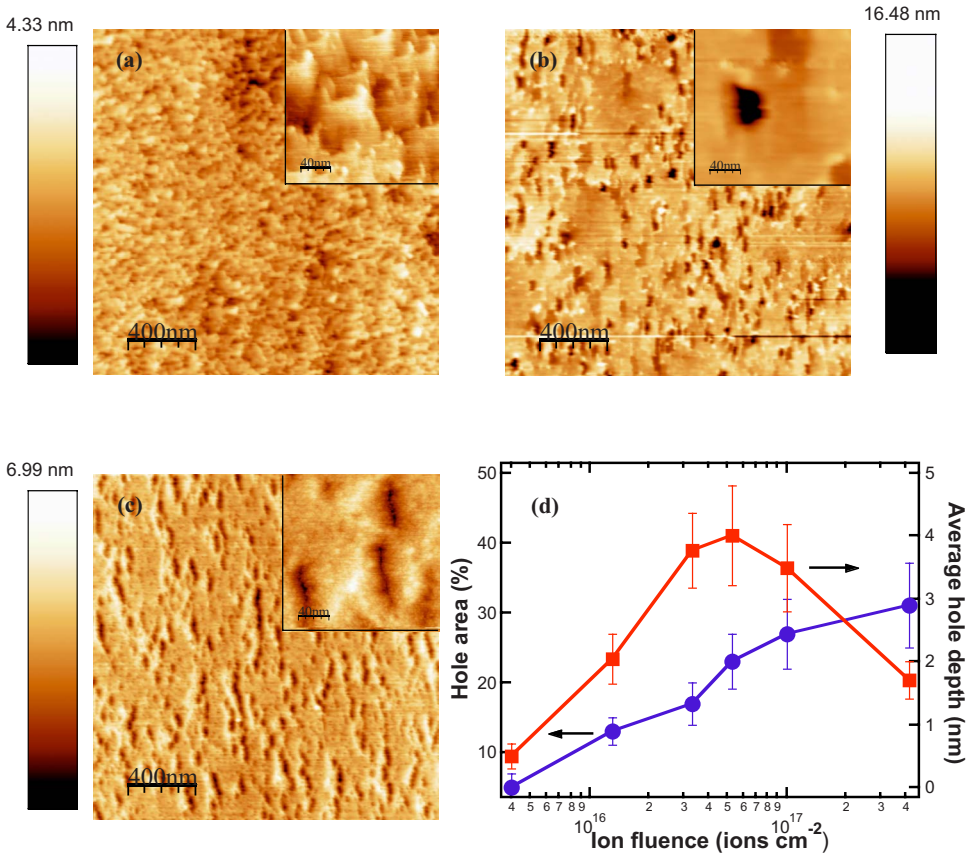

FIG. 1. (Color online) STM topography of $TiO_2(110)$ (a) Virgin surface; after sputtering with 0.5 keV Ar^+ at (b) 3.3×10^{16} and (c) 4.2×10^{17} ions cm^{-2}; and (d) the percentage of the surface covered by holes and the average hole depth given as a function of ion fluence. A color scale indicating the depth in the images is shown to the left of each topograph. Each topograph also contains a high-resolution inset detailing a typical small feature.

that the average roughness of the starting surface was measured from the images to be 0.4 nm. It increases to about 2 nm at a fluence of 6×10^{16} ions cm^{-2} and then decreases following additional bombardment. Such a simple calculation of surface roughness is not meaningful, however, as the surface features are not Gaussian.

Figure 2 shows Ti $2p$ XPS spectra for $TiO_2(110)$ collected after each sputtering cycle, and then after the postannealing. The $2p_{3/2}$ binding energies for different oxidation states are depicted by vertical lines.[19,20] Only the Ti^{4+} component is present on the virgin surface, while Ti^{3+} and Ti^{2+} emerge with sputtering. At the highest Ar^+ fluence, the Ti^{4+} component has vanished. The appearance of Ti^{3+} and Ti^{2+}, in addition to Ti^{4+}, was previously reported for $TiO_2(100)$ bombarded by 2 keV Ar^+.[21] Note that there is no evidence in the spectra for fully reduced Ti metal at any fluence or post annealing temperature.

The O 1s level decreases in intensity and shifts slightly to higher binding energy with ion bombardment (spectra not shown). The inset in Fig. 2 shows the intensity ratio of the oxygen to titanium photoelectron signals as a function of ion fluence, after normalizing by the photoionization cross sections.[22] The ratio of the starting surface is slightly less than stoichiometric, as expected, but it decreases considerably with sputtering. Oxygen is preferentially sputtered due to its lower mass, and the initial fast decrease suggests that

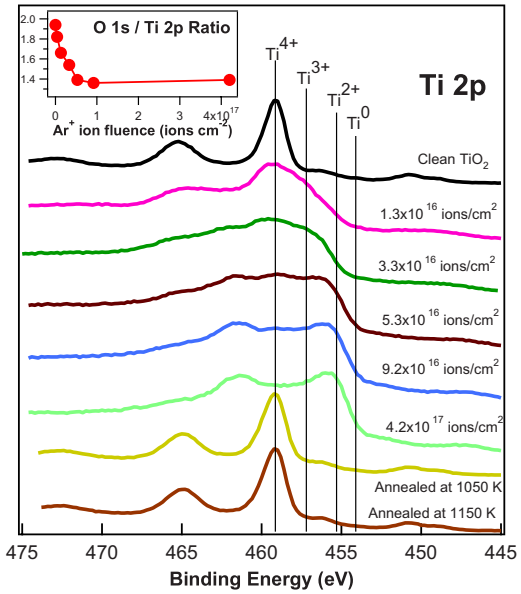

FIG. 2. (Color online) Ti $2p$ XPS spectra collected after sputtering at different Ar^+ fluences, and postannealing. The inset shows the O 1s to Ti $2p$ ratio, normalized by photoelectron cross section, as a function of ion fluence.

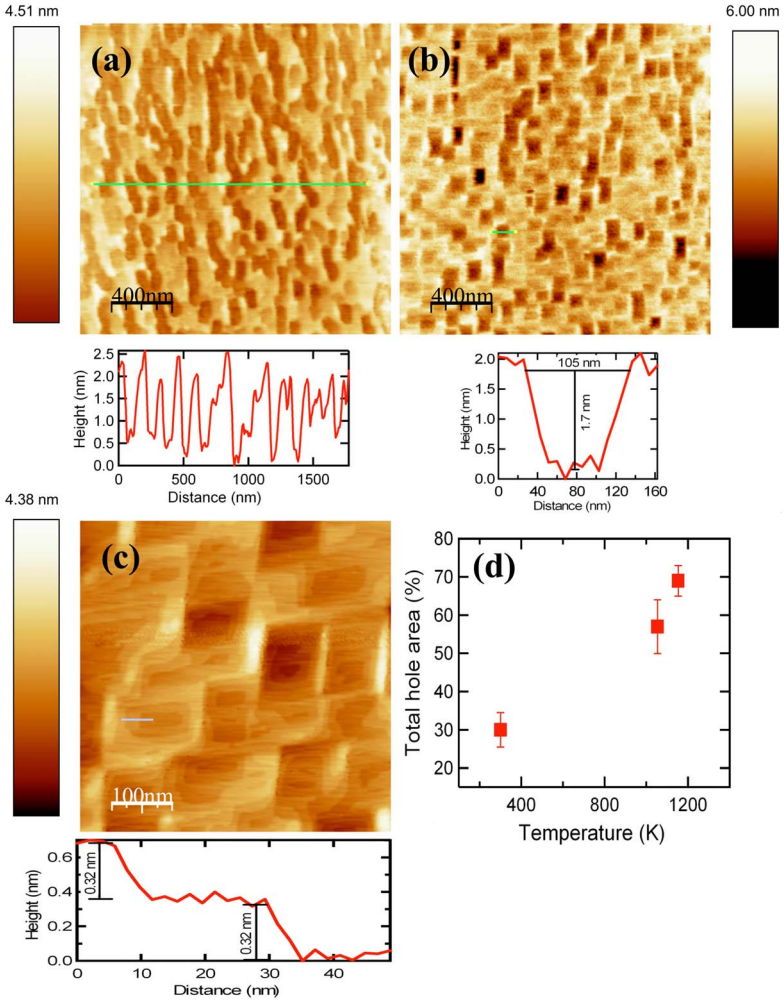

FIG. 3. (Color online) STM topography of TiO_2 after prolonged ion sputtering (4.2×10^{17} ions cm^{-2}) followed by annealing at (a) 1050 and (b) 1150 K; (c) closeup view of rectangular vacancy clusters where single atomic layers are visible; (d) percentage of the surface occupied by vacancies shown as a function of annealing temperature. A line scan collected from the indicated portion is shown below each image in (a), (b), and (c).

the oxygen atoms from the outermost layer are the first to be removed. This was also seen for TiO_2 by Pan *et al.* when they measured the stoichiometry of the sputtered material with XPS and LEIS.[9]

The ion-induced growth of nanocavities and the morphology of heavily sputtered surfaces are often described by the Bradley and Harper (BH) linear theory[23] with its nonlinear extension.[24] The probability that a surface atom is ejected is proportional to the energy transferred by the collision cascade. The BH model predicts that the total energy deposited, and therefore the number of sputtered atoms, is sensitive to the local surface curvature. Surface atoms are removed preferentially from valleys, whereas emission from ridges is inhibited, which leads to enhancement of the local curvature and thus the formation of self-organized nanostructures. Recently, an extension of the BH linear theory described prolonged sputtering effects and ion induced diffusion phenomena.[13,24] Most of the theoretical and experimental studies of ion-induced surface morphology have concentrated on the curvature-dependent erosion, nonlinear erosion, and diffusion phenomena, and have neglected the initiation of the process. Cuerno *et al.*[24] introduced a noise term to consider the random arrival of the ions, but the effect of the noise term on surface morphology was not emphasized. Khang *et al.*[27] did not consider the noise term, and instead assumed an initially rough surface for their simulations of ion-induced hole and dot formation.

The initiation of ion-induced structure formation on TiO_2 by Ar^+ ion impact can be described by the random and discrete arrival of ions and the preferential sputtering of oxygen. The flux in the present experiment is 6.2×10^{12} ions cm^{-2} s^{-1}, so that, on average, one ion is incident in a 16 nm^2 surface area per second. The lateral extension of the collision cascade for a 0.5 keV Ar^+ ion in TiO_2 is $\sim$1 nm,[25] and the lifetime of a collision cascade is on the order of 10^{-13}–10^{-12} s.[26] Thus, overlap of collision cascades initiated by sequentially implanted ions is extremely rare and ion impact can be considered as a discrete process. The preferential sputtering of oxygen initiates instabilities in the form of random atomic vacancies, primarily of oxygen, which are created at the onset of sputtering. This initial defect formation disrupts the flatness of the surface. Once the flatness of the surface is broken, curvature dependent sputtering beings, which leads to enhancement of the craters. An increase of the hole area and the average hole depth with sputtering fluence is thus observed. The resulting morphology, however, is not Gaussian as there are large flat areas separated by craters [Figs. 1(b) and 1(c)].

It is thus clear that the BH model by itself cannot account for the structures observed here. A likely reason is that, in

addition to the removal of atoms during sputtering, diffusion of adatoms and vacancies plays a vital role in determining the surface morphology even at room temperature. Thus, a combination of the removal of atoms and diffusion of the generated vacancies and adatoms acts to form the self-organized vacancy clusters (Fig. 1). The diffusion could be either ion-beam induced or thermal. In Fig. 1(d), it is shown that the average cavity depth decreases following prolonged ion bombardment. A likely explanation is that the vacancy clusters extend below the surface, and thus only parts of the cavities are imaged by STM.

In order to investigate the effects of thermal diffusion of the sputter-induced vacancies, a sample that was subjected to prolonged ion bombardment was subsequently annealed in vacuum. Figure 3(a) shows the morphology after sputtering at a fluence of 4.2×10^{17} ions cm^{-2} and subsequent annealing at 1050 K. The formation of nearly periodic structures is seen in the image and line scan data. After annealing at 1150 K, the vacancies become regular rectangular cavities, with typical lengths of 85 nm and depths of 3.3 nm [Fig. 3(b)]. In Fig. 3(d), it is seen that the ratio of vacancy to total surface area increases with annealing temperature to a value well above what is obtained from prolonged sputtering at room temperature. From the XPS data (Fig. 2), it is seen that Ti^{4+} reappears after annealing above 1050 K, indicating recovery of the initial stoichiometry. Note that similar rectangular-shaped cavities, with sizes of 50–100 nm, were observed on $TiO_2(001)$ after photoetching.[4] A complicated network structure was also observed after sputtering and annealing $TiO_2(001)$.[28]

High-temperature annealing increases the mobility of the adatoms and vacancies generated by the ion bombardment. After prolonged bombardment, the surface and subsurface layers contain random and irregularly shaped vacancies. At an elevated temperature (1050 K) the thermal diffusion is activated, which leads to coalescence of the vacancies to form larger vacancy clusters, thus increasing the total vacancy area. Along with the diffusion of vacancies, the increased temperature induces the diffusion of oxygen atoms from the bulk to the surface so that the TiO_2 recovers its stoichiometry.

The shape of the regular rectangular cavities that appear following the 1150 K anneal can be understood by considering the ion-induced cavities and the diffusion of atoms across steps following their reappearance. Figure 3(c) shows a closeup of the rectangular vacancy clusters with single atomic steps (0.32 nm). At this temperature, the atoms diffuse along the energetically favored direction and attempt to resurrect the ordered surface centering on the cavities. It is likely that there is a barrier to diffusion at the step edges, such as an Ehrlich-Schwoebel barrier,[13,29] so that the diffusing atoms are restricted from descending and filling up the cavities, resulting in rectangular vacancy clusters. Whatever the cause, however, it is clear that diffusion plays a large role in the formation of these ion-induced structures.

In summary, it is shown that low-energy Ar^+ ion beams provide a simple and efficient method for producing atomic- and nanometer-size defects on a $TiO_2(110)$ surface. Instabilities, such as preferential sputtering and the random arrival of ions, along with curvature-dependent sputtering and vacancy or adatom diffusion, are all involved in determining the surface topography following room-temperature sputtering. After prolonged sputtering and high-temperature annealing, the TiO_2 stoichiometry is recovered with nanometer-scale rectangular vacancy cluster formation, which suggests that the substrate temperature could be used as a parameter for achieving a regular periodic surface pattern following ion bombardment.

This material is based upon work supported by, or in part by, the U.S. Army Research Laboratory and U.S. Army Research Office (Contract No. 46686-PH-H).

*Present address: Radioactive Ion Beam Division, Variable Energy Cyclotron Centre, 1/AF, Bidhannagar, Kolkata 700 064, India.
†Corresponding author. yarmoff@ucr.edu

[1] J. Nowotny *et al.*, J. Phys. Chem. B **110**, 18492 (2006).
[2] E. Wahlström *et al.*, Phys. Rev. Lett. **90**, 026101 (2003).
[3] J. Abad *et al.*, Surf. Sci. **549**, 134 (2004).
[4] K. Hashimoto *et al.*, Jpn. J. Appl. Phys., Part 1 **44**, 8269 (2005).
[5] M. A. Barteau, Chem. Rev. (Washington, D.C.) **96**, 1413 (1996).
[6] U. Diebold *et al.* Surf. Sci. **411**, 137 (1998).
[7] R. Schaub *et al.* Science **299**, 377 (2003).
[8] S. Petigny *et al.*, Surf. Sci. **410**, 250 (1998).
[9] J.-M. Pan *et al.*, J. Vac. Sci. Technol. A **10**, 2470 (1992).
[10] V. S. Lusvardi *et al.*, J. G. Chen, Surf. Sci. **397**, 237 (1998).
[11] M. A. Henderson, Surf. Sci. **419**, 174 (1999).
[12] T. Michely and C. Teichert, Phys. Rev. B **50**, 11156 (1994).
[13] U. Valbusa *et al.*, J. Phys.: Condens. Matter **14**, 8153 (2002).
[14] A. Berko *et al.*, Appl. Surf. Sci. **246**, 174 (2005).
[15] C. M. Wang *et al.*, Phys. Rev. B **72**, 245421 (2005).
[16] P. Karmakar *et al.*, Phys. Rev. Lett. **98**, 215502 (2007).
[17] U. Diebold, Surf. Sci. Rep. **48**, 53 (2002).
[18] S. Fischer *et al.*, J. Vac. Sci. Technol. B **14**, 961 (1996).
[19] J. F. Moulder and W. F. Stickle, *Handbook of X-ray Photoelectron Spectroscopy* (Perkin-Elmer, Physical Electronics Division, Eden Prairie, 1992).
[20] J. Mayer *et al.*, J. Electron Spectrosc. Relat. Phenom. **73**, 1 (1995).
[21] S. Hashimoto *et al.*, Surf. Sci. **556**, 22 (2004).
[22] J. J. Yeh and I. Lindau, At. Data Nucl. Data Tables **32**, 1 (1985).
[23] R. M. Bradley and J. M. E. Harper, J. Vac. Sci. Technol. A **6**, 2390 (1988).
[24] R. Cuerno and A.-L. Barabási, Phys. Rev. Lett. **74**, 4746 (1995).
[25] J. Ziegler *et al.*, *The Stopping and Range of Ions in Solids* (Pergamon, New York, 1985).
[26] W. Möller, http://www.fz-rossendorf.de/FWI
[27] S. Park *et al.*, Phys. Rev. Lett. **83**, 3486 (1999).
[28] K. Fukui *et al.*, Jpn. J. Appl. Phys., Part 1 **40**, 4331 (2001).
[29] P. Politi and J. Villain, Phys. Rev. B **54**, 5114 (1996).